Research Square

Preprints are preliminary reports that have not undergone peer review.
They should not be considered conclusive, used to inform clinical practice,
or referenced by the media as validated information.

Daily CBCT-Based Repeated-Measures Analysis of Setup Reproducibility and Treatment-Course Stability of Three Positioning–Immobilization Strategies in Cervical Cancer VMAT

Zhiyue Lin
Sun Yat-sen University Cancer Center
Hailong Wang
Sun Yat-sen University Cancer Center
Yingnan Qi
Sun Yat-sen University Cancer Center
Kai Wang
Sun Yat-sen Memorial Hospital, Sun Yat-sen University
Jiaxiu Luo
Sun Yat-sen University Cancer Center
Zongtai Li
Sun Yat-sen University Cancer Center
Bin Zhang
Sun Yat-sen University Cancer Center
Senkui Xu
Sun Yat-sen University Cancer Center
Huilang He
Sun Yat-sen University Cancer Center
Feng Chi
Sun Yat-sen University Cancer Center
Wenlong Zhu
zhuwl@sysucc.org.cn

Sun Yat-sen University Cancer Center

Research Article

Keywords: Cervical cancer, cone-beam computed tomography, image-guided radiotherapy, volumetric modulated arc therapy, immobilization, setup reproducibility

Posted Date: November 19th, 2026

DOI: https://doi.org/10.21203/rs.3.rs-11630466/v1

License: This work is licensed under a Creative Commons Attribution 4.0 International License.
Read Full License

Additional Declarations: No competing interests reported.

Daily CBCT-Based Repeated-Measures Analysis of Setup Reproducibility and Treatment-Course Stability of Three Positioning–Immobilization Strategies in Cervical Cancer VMAT

Zhiyue Lin1†, Hailong Wang1†, Yingnan Qi1†, Kai Wang2, Jiaxiu Luo1, Zongtai Li1, Bin Zhang1, Senkui Xu1, Huilang He1*, Feng Chi1*, Wenlong Zhu1*

1 Department of Radiation Oncology, State Key Laboratory of Oncology in South China, Guangdong Provincial Clinical Research Center for Cancer, Sun Yat-sen University Cancer Center, Guangzhou, China

2 Sun Yat-sen Memorial Hospital, Sun Yat-sen University, Guangzhou, China

† Zhiyue Lin, Hailong Wang, and Yingnan Qi contributed equally to this work.

Correspondence:

Huilang He

Email: hehl@sysucc.org.cn

Feng Chi

Email: chifeng@sysucc.org.cn

Wenlong Zhu

Email: zhuwl@sysucc.org.cn

* Corresponding authors:

Huilang He

Feng Chi

Wenlong Zhu

Abstract

Background

Accurate and reproducible patient positioning is essential for image-guided radiotherapy (IGRT) in cervical cancer. This study compared pretreatment setup reproducibility and treatment-course changes among three positioning–immobilization strategies using daily cone-beam computed tomography (CBCT) and repeated-measures analysis.

Methods

This retrospective study included 255 patients undergoing volumetric modulated arc therapy (VMAT) for cervical cancer: Group A, supine positioning with vacuum-cushion immobilization (n = 100); Group B, prone positioning with an Orfit body frame and thermoplastic fixation (n = 100); and Group C, prone positioning with an individualized belly-board system (n = 55). A total of 6,255 daily pretreatment CBCT registrations were analyzed. Pre-correction translational setup deviations in the longitudinal (LNG), lateral (LAT), and vertical (VRT) directions and the corresponding three-dimensional (3D) vector magnitude were evaluated. Generalized estimating equation (GEE) models accounted for within-patient correlation, with multivariable adjustment for age, body mass index, and irradiation field extent. Patient-level sensitivity analyses, descriptive setup-related uncertainty estimates, and threshold-based reproducibility analyses requiring simultaneous attainment in all three translational directions were also performed.

Results

In adjusted GEE analysis, 3D vector magnitude was greater in Group B (β = 0.0647 cm; 95% CI, 0.0077–0.1217; P = 0.026) and Group C (β = 0.1038 cm; 95% CI, 0.0342–0.1734; P = 0.003) than in Group A. Treatment fraction number was positively associated with 3D vector magnitude (β = 0.0032 cm/fraction; P < 0.001), without significant group-by-fraction interactions. Patient-level sensitivity analyses supported the overall between-group pattern. Direction-specific analyses showed greater longitudinal deviations in Group B and greater vertical deviations in Group C. Under the strict patient-level criterion requiring all three absolute directional deviations to remain ≤0.5 cm at every available CBCT verification, attainment rates were 43.0%, 28.0%, and 12.7% in Groups A, B, and C, respectively (P < 0.001).

Conclusions

The three positioning–immobilization strategies exhibited distinct patterns of pre-correction setup deviations during daily CBCT-guided VMAT for cervical cancer. Supine positioning with vacuum-cushion immobilization was associated with smaller 3D setup deviations and higher descriptive threshold-attainment rates than the two prone strategies in this cohort. These findings reflect pretreatment setup reproducibility rather than isolated immobilization-device performance, post-correction treatment accuracy, or recommended

clinical planning margins.

Keywords

Cervical cancer; cone-beam computed tomography; image-guided radiotherapy; volumetric modulated arc therapy; immobilization; setup reproducibility.

1 Introduction

Cervical cancer remains one of the most common malignancies among women worldwide and continues to pose a substantial public health burden despite advances in human papillomavirus vaccination, screening programs, and multidisciplinary treatment strategies [1,2]. Radiotherapy plays a pivotal role in cervical cancer management across different disease stages. Concurrent chemoradiotherapy is a standard treatment for locally advanced disease, whereas postoperative radiotherapy is recommended for selected patients with adverse pathological risk factors [3]. Advances in volumetric modulated arc therapy (VMAT) have improved dose conformity and organ-at-risk sparing, while image-guided radiotherapy (IGRT) has enhanced the accuracy of treatment positioning and delivery [4].

The precision of modern radiotherapy depends not only on advanced treatment planning and delivery techniques but also on reproducible patient positioning throughout the treatment course. Cervical cancer radiotherapy frequently involves pelvic or extended-field irradiation, during which interfraction variations may arise from changes in bladder filling, rectal distension, body contour, patient relaxation, and positioning reproducibility [5]. Such variations contribute to geometric uncertainty and, if not adequately corrected, may compromise treatment delivery. Therefore, minimizing setup uncertainty through reproducible positioning, appropriate immobilization, and image guidance remains essential for high-quality radiotherapy [6].

Daily cone-beam computed tomography (CBCT) is an important component of IGRT, enabling the assessment and online correction of interfraction setup deviations before treatment delivery [7,8]. Pre-correction CBCT registrations also provide quantitative information on translational setup deviations, including directional and

absolute deviations, three-dimensional (3D) vector magnitude, and systematic and random components of setup uncertainty [9,10]. Setup-related margin estimates derived from these measurements may provide additional comparative information regarding geometric uncertainty but should be distinguished from post-correction residual errors and clinically applied clinical target volume-to-planning target volume (CTV-to-PTV) margins in a daily image-guided workflow. Moreover, because daily CBCT generates repeated measurements from the same patient, statistical comparisons of positioning–immobilization strategies should account for within-patient correlation. Treating individual CBCT registrations as independent observations may lead to inappropriate statistical inference.

Several positioning–immobilization strategies are used in cervical cancer radiotherapy, including supine positioning with vacuum-cushion immobilization, prone positioning with an Orfit body frame and thermoplastic fixation, and prone positioning with individualized belly-board systems [11]. These strategies differ in treatment position, support configuration, and patient–device contact. Supine positioning with vacuum-cushion immobilization provides individualized body-contour support, whereas the Orfit-based strategy combines prone positioning with structured body support and thermoplastic fixation. The individualized belly-board strategy uses prone positioning with individualized abdominal and pelvic support. These distinct configurations may be associated with different patterns of setup reproducibility throughout the treatment course. Although previous studies have evaluated supine and prone positioning or individual immobilization approaches, comparative evidence integrating large daily-CBCT datasets with repeated-measures analysis remains limited [12, 13].

Therefore, this retrospective study analyzed 6,255 daily pretreatment CBCT registrations from 255 patients with cervical cancer treated with VMAT using three positioning–immobilization strategies. Generalized estimating equation (GEE) models were used to account for within-patient correlation across repeated treatment fractions, with additional adjustment for available patient- and treatment-related covariates. Patient-level sensitivity analyses were performed to assess the robustness of the

findings. The study aimed to compare pre-correction setup reproducibility among the three strategies and to characterize systematic and random setup uncertainty, descriptive setup-related margin estimates, longitudinal changes across treatment fractions, and treatment-course reproducibility based on simultaneous three-directional threshold attainment.

2. Materials and Methods

2.1 Study Design and Patient Population

This single-center retrospective cohort study included consecutive patients with cervical cancer who underwent VMAT at Sun Yat-sen University Cancer Center between December 2020 and May 2025.

Patients were eligible if they met the following criteria: (1) pathologically confirmed primary cervical cancer; (2) treatment with VMAT; (3) pretreatment CBCT verification before each treatment fraction; and (4) availability of complete clinical, treatment, and imaging data required for the present analysis. Patients were excluded if CBCT registration records were incomplete, essential clinical or treatment data were unavailable, or the prescribed radiotherapy course was not completed.

A total of 255 consecutive patients were included, contributing 6,255 daily pretreatment CBCT registrations. The patient was considered the unit of enrollment, whereas individual treatment fractions represented repeated observations within the same patient. According to the positioning and immobilization strategy used in routine clinical practice, patients were classified into three groups: supine positioning with vacuum-cushion immobilization (Group A, n = 100), prone positioning using an Orfit body frame with thermoplastic fixation (Group B, n = 100), and prone positioning using an individualized belly-board system (Group C, n = 55). Because both patient position and immobilization method differed among the groups, these groups were considered combined positioning–immobilization strategies rather than isolated immobilization-device categories.

The primary outcome was the three-dimensional (3D) vector magnitude calculated from pre-correction CBCT-derived translational setup deviations.

Secondary outcomes included signed and absolute translational setup deviations in the longitudinal (LNG), lateral (LAT), and vertical (VRT) directions; systematic and random setup errors; setup-related margin estimates; longitudinal changes in setup deviations across treatment fractions; and treatment-course reproducibility measures. Age, body mass index (BMI), irradiation field extent, and prescription dose were collected as patient- or treatment-related covariates. Treatment fraction number was recorded for each CBCT observation and was included in the repeated-measures analysis to evaluate longitudinal changes in setup deviation. Detailed definitions of the CBCT-derived setup deviations and outcome measures are provided in Sections 2.4 and 2.5, respectively.

The study was approved by the Ethics Committee of Sun Yat-sen University Cancer Center (Approval No. SL-B2024-773-02) and was conducted in accordance with the Declaration of Helsinki. The requirement for informed consent was waived because of the retrospective study design.

2.2 CT Simulation and Treatment Planning

All patients underwent computed tomography (CT) simulation using a 64-slice large-bore CT scanner (Brilliance CT Big Bore; Philips Healthcare, Best, the Netherlands).

A standardized bowel and bladder preparation protocol was implemented at CT simulation and subsequently followed before each treatment fraction. For CT simulation, patients were instructed to empty the rectum and bladder and subsequently drink 500 mL of water. CT acquisition was performed after the bladder volume reached 250 – 350 mL, as confirmed using an ultrasound bladder scanner.

Both non-contrast and contrast-enhanced CT images were acquired for treatment planning. Non-contrast CT images were obtained at 140 kVp with a 5-mm slice thickness and a 600-mm field of view. Contrast-enhanced CT images were acquired at 120 kVp following intravenous administration of iomeprol 350 at a rate of 2.0 – 2.5 mL/s, with an 80-s scan delay. The scan range extended from the tenth thoracic vertebra to 3 cm below the ischial tuberosities.

The CT datasets were imported into the Monaco treatment planning system

(Elekta AB, Stockholm, Sweden). Target volumes and organs at risk were delineated by experienced radiation oncologists, and VMAT plans were generated and reviewed by qualified medical physicists according to institutional clinical protocols.

2.3 Positioning and Immobilization Strategies

Three positioning–immobilization strategies were used in routine clinical practice according to patient characteristics, treatment position, and institutional workflow. Because both treatment position and immobilization method differed among the three groups, the strategies were evaluated as combined positioning–immobilization approaches rather than as isolated effects of individual immobilization devices.

Group A: Supine positioning with vacuum-cushion immobilization

Patients were positioned supine on a customized 1.2-m vacuum cushion with both arms raised above the head. The vacuum cushion was individually molded under negative pressure to provide reproducible support for the shoulders, trunk, pelvis, and lower extremities.

Group B: Prone positioning with an Orfit body frame and thermoplastic fixation

Patients were positioned prone on an Orfit body frame, with the abdomen positioned over the abdominal opening. The lower abdomen and pelvis were immobilized using an individualized thermoplastic fixation system. The abdominal opening and pelvic support were adjusted according to the patient's body habitus.

Group C: Prone positioning with an individualized belly-board system

Patients were positioned prone on an individualized belly-board system, with both hands placed on the hand grips and the feet secured using foot supports. The abdomen was allowed to descend naturally into the abdominal opening, and an individualized vacuum support cushion was used to support the abdominopelvic region.

Representative positioning and immobilization strategies are shown in Figure 1.



Figure 1. Representative positioning and immobilization strategies used in this

study.

(A) Supine positioning with vacuum-cushion immobilization.

(B) Prone positioning with an Orfit body frame and thermoplastic fixation.

(C) Prone positioning with an individualized belly-board system.

2.4 Daily Treatment Workflow and CBCT Image Guidance

All patients followed the same standardized bowel and bladder preparation protocol before each treatment fraction to promote consistency in rectal emptying and bladder filling throughout the radiotherapy course. Initial patient positioning was performed using room lasers, skin tattoos, immobilization reference marks, and couch coordinates recorded during CT simulation. The corresponding positioning–immobilization strategy was reproduced according to the simulation setup at each treatment fraction.

Daily pretreatment CBCT was acquired for each treatment fraction using the on-board imaging system integrated with the linear accelerator. CBCT images were reconstructed with a slice thickness of 5 mm. Image registration was performed using three translational degrees of freedom in the LNG, LAT, and VRT directions; rotational registration and correction were not routinely performed. Automatic registration between the CBCT images and planning CT was initially performed using the routine clinical registration workflow. The registration result was subsequently reviewed with reference to the planning target volume (PTV), relevant soft-tissue anatomy, and pelvic bony structures. When the automatic registration was considered unsatisfactory, manual refinement was performed by the radiation therapists. The final registration was jointly confirmed by two radiation therapists before treatment delivery.

Translational deviations from the final pretreatment CBCT-to-planning-CT registration were recorded before couch correction. In the present study, these values were defined as pre-correction CBCT-derived translational setup deviations obtained from routine clinical registration and were subsequently used to guide translational couch corrections before treatment delivery. Routine repeat CBCT after couch correction was not performed; therefore, the analyzed shifts represent pre-correction

setup deviations rather than post-correction residual setup errors.

Because the routine clinical registration procedure incorporated information from the PTV, relevant soft-tissue anatomy, and pelvic bony structures rather than relying exclusively on bone-only registration, the recorded translational deviations may reflect both external positioning variation and internal anatomical variation. Accordingly, these measurements were interpreted as CBCT-derived pretreatment setup deviations and not as a pure measure of immobilization-device reproducibility.

Each patient contributed multiple daily pretreatment CBCT registrations during the radiotherapy course, resulting in longitudinal repeated measurements. Statistical analyses therefore accounted for within-patient correlation across treatment fractions.

2.5 Outcome Measures

The primary outcome was the three-dimensional (3D) vector magnitude derived from the pre-correction CBCT-derived translational setup deviations obtained from routine clinical registration. Directional setup deviations were recorded as signed values in the LNG, LAT, and VRT directions. Absolute directional deviations were calculated as |LNG|, |LAT|, and |VRT|. The 3D vector magnitude was calculated as:

$$\mathrm{3D\ vector\ magnitude}=\sqrt{LNG^2+LAT^2+VRT^2}.$$

Secondary outcomes included signed and absolute directional setup deviations, systematic error (Σ), random error (σ), descriptive setup-related margin estimates, longitudinal changes in setup deviations across treatment fractions, and treatment-course reproducibility measures.

Treatment-course reproducibility was descriptively evaluated using predefined 3D vector-magnitude thresholds of ≤0.5 cm and ≤1.0 cm. For each patient, the fraction pass rate was calculated as the proportion of available treatment fractions in which the 3D vector magnitude met the corresponding threshold. A strict patient-level criterion, defined as meeting the corresponding threshold at every available pretreatment CBCT verification throughout the treatment course, was retained as a descriptive measure only. Patient-level mean absolute directional deviations, mean 3D vector magnitude, and the 95th percentile of the 3D vector magnitude were also calculated.

2.6 Statistical Analysis

Continuous variables were summarized as mean ± standard deviation (SD) or median with interquartile range (IQR), as appropriate, and categorical variables as frequencies and percentages. Baseline patient and treatment characteristics were compared among the three positioning–immobilization groups using one-way analysis of variance or the Kruskal–Wallis test for continuous variables, as appropriate, and the chi-square test or Fisher's exact test for categorical variables.

Because each patient contributed multiple daily CBCT measurements, generalized estimating equation (GEE) models were used to account for within-patient correlation across treatment fractions. GEE models were specified with a Gaussian distribution, identity link function, exchangeable working correlation structure, and robust standard errors. The three-dimensional (3D) vector magnitude was specified as the primary outcome, with positioning–immobilization strategy as the primary explanatory variable and Group A (supine positioning with vacuum-cushion immobilization) as the reference group. Group A was selected as the reference because it represented the supine positioning strategy and provided a clinically relevant comparator for the two prone positioning–immobilization strategies. Treatment fraction number was included as a continuous variable to evaluate longitudinal changes in setup deviation over the radiotherapy course. Group-by-fraction interaction terms were additionally examined to assess whether longitudinal changes differed among the three positioning–immobilization strategies.

To address potential confounding associated with the non-randomized retrospective design, multivariable GEE models were additionally adjusted for age, body mass index (BMI), and irradiation field extent. These covariates were selected based on their clinical relevance and availability in the retrospective dataset. Irradiation field extent was categorized as extended-field or non-extended-field irradiation according to the recorded superior field border. Because BMI data were not available for all patients, the multivariable adjusted GEE analysis was performed as a complete-case analysis including patients with available data for all included covariates. Regression coefficients (β) with 95% confidence intervals (CIs) and

corresponding P values were reported.

Patient-level sensitivity analyses were performed by aggregating repeated CBCT measurements within each patient. Patient-specific mean absolute deviations in the longitudinal (LNG), lateral (LAT), and vertical (VRT) directions, mean 3D vector magnitude, and the 95th percentile of the 3D vector magnitude were calculated and compared among the three groups using the Kruskal–Wallis test.

Treatment-course setup reproducibility was further evaluated using two complementary threshold-based measures. A fraction was considered to meet the specified threshold when the absolute translational deviations in all three directions (LNG, LAT, and VRT) simultaneously satisfied the ≤0.5-cm or ≤1.0-cm criterion. Strict patient-level attainment required this criterion to be met at every available pretreatment CBCT verification throughout the treatment course. The patient-specific fraction pass rate was defined as the percentage of available treatment fractions meeting the corresponding criterion for each patient. Strict patient-level attainment proportions were compared using the chi-square test or Fisher's exact test, as appropriate, whereas patient-specific fraction pass rates were compared using the Kruskal–Wallis test. These thresholds were used as descriptive benchmarks rather than clinical action levels or recommended setup tolerances.

For each translational direction, the systematic error (Σ) was defined as the standard deviation of the patient-specific mean setup deviations, whereas the random error (σ) was calculated as the root-mean-square of the patient-specific standard deviations. Setup-related margin estimates were calculated using the van Herk formula:

[M = 2.5\Sigma + 0.7\sigma.]

Because these estimates were derived from pre-correction CBCT-derived translational setup deviations obtained from routine clinical registration, they were interpreted as descriptive comparative measures of setup-related geometric uncertainty rather than as recommended clinical clinical target volume-to-planning target volume (CTV-to-PTV) margins for a daily image-guided workflow. These estimates do not account for post-correction residual errors, rotational errors,

intrafraction motion, or target-specific internal anatomical variation.

All statistical tests were two-sided, and a P value <0.05 was considered statistically significant. Statistical analyses were performed using IBM SPSS Statistics version 27.0 (IBM Corp., Armonk, NY, USA).

3. Results

3.1 Patient and Treatment Characteristics

A total of 255 patients with cervical cancer were included, contributing 6,255 daily pretreatment CBCT registrations. According to the positioning–immobilization strategy used in routine clinical practice, 100 patients underwent supine positioning with vacuum-cushion immobilization (Group A), 100 underwent prone positioning with an Orfit body frame and thermoplastic fixation (Group B), and 55 underwent prone positioning with an individualized belly-board system (Group C).

Baseline patient and treatment characteristics are summarized in Table 1. Age and BMI were comparable among the three groups (P = 0.528 and P = 0.495, respectively). BMI data were available for 206 patients (80.8%), with significant differences in BMI availability among the groups (P = 0.001). The distribution of irradiation field extent also differed among the groups (P = 0.015). Overall, the median number of CBCT registrations per patient was 25 (IQR, 24–25).

Table 1. Baseline patient and treatment characteristics according to positioning–immobilization strategy

Characteristic	Group A Supine vacuum cushion (n=100)	Group B Prone Orfit body frame (n=100)	Group C Individualized prone belly-board (n=55)	Overall (N=255)	P value
Patient characteristics					
Age, years	54.9 ± 11.7	53.1 ± 10.5	54.5 ± 10.5	54.1 ± 11.0	0.528

BMI, kg/m²	23.2(21.3–25.1)	23.5(20.8–25.5)	23.7(21.1–26.3)	23.4(21.0–25.6)	0.495
BMI available, n/N (%)	69/100 (69.0%)	89/100 (89.0%)	48/55 (87.3%)	206/255 (80.8%)	0.001
Treatment characteristics					
Irradiation field extent					0.015
Extended-field irradiation	63 (63.0%)	77 (77.8%)	45 (81.8%)	185(72.8%)	
Non-extended-field irradiation	37 (37.0%)	22 (22.2%)	10 (18.2%)	69 (27.2%)	
Missing field extent	0	1 (1.0%)	0	1 (0.4%)	
CBCT dataset characteristic					
No. of CBCT registrations	2,436	2,468	1,351	6,255	—
CBCT registrations per patient	25 (24–25)	25 (25–25)	25 (24–25)	25 (24–25)	0.007

Footnote: Data are presented as mean ± standard deviation, median (interquartile range), or n/N (%), as appropriate. Age, BMI, and CBCT registrations per patient were compared using the Kruskal–Wallis test; categorical variables were compared

using the chi-square test. BMI and irradiation field extent were available for 206 and 254 patients, respectively. Percentages for irradiation field extent were calculated using available data. BMI, body mass index; CBCT, cone-beam computed tomography.

3.2 Unadjusted Record-Level CBCT-Derived Setup Deviations

Descriptive statistics of pre-correction CBCT-derived translational setup deviations from all 6,255 pretreatment CBCT registrations are presented in Table 2 and Figures 2 and 3.

For signed directional deviations, the mean longitudinal (LNG) deviations were 0.152 ± 0.375 cm, −0.256 ± 0.451 cm, and 0.012 ± 0.438 cm in Groups A, B, and C, respectively. Group B exhibited the largest negative mean LNG deviation. In the lateral (LAT) direction, the corresponding deviations were 0.008 ± 0.354 cm, −0.004 ± 0.312 cm, and 0.132 ± 0.295 cm, with Group C showing the largest positive mean deviation. In the vertical (VRT) direction, the mean deviations were 0.036 ± 0.311 cm, −0.068 ± 0.332 cm, and −0.131 ± 0.493 cm, respectively, with Group C exhibiting the largest negative mean deviation.

For absolute directional deviations, the mean absolute LNG deviations were 0.321 ± 0.246 cm, 0.412 ± 0.314 cm, and 0.341 ± 0.275 cm in Groups A, B, and C, respectively, with the highest value observed in Group B. The corresponding mean absolute LAT deviations were 0.264 ± 0.237 cm, 0.240 ± 0.199 cm, and 0.239 ± 0.218 cm, showing similar magnitudes across the three groups. Mean absolute VRT deviations were 0.246 ± 0.195 cm, 0.266 ± 0.211 cm, and 0.385 ± 0.335 cm, respectively, with the highest value observed in Group C.

The mean three-dimensional (3D) vector magnitude was 0.558 ± 0.275 cm in Group A, 0.626 ± 0.299 cm in Group B, and 0.659 ± 0.350 cm in Group C. Group A showed the lowest mean 3D vector magnitude, followed by Groups B and C.

Overall, the descriptive results showed distinct directional patterns of setup deviations across the three positioning–immobilization strategies.

Table 2. Unadjusted record-level setup-error characteristics according to

positioning–immobilization strategy

Setup-deviation parameter	Group A (n=2,436)	Group B (n=2,468)	Group C (n=1,351)
Signed directional errors, cm			
LNG	0.152 ± 0.375	−0.256 ± 0.451	0.012 ± 0.438
LAT	0.008 ± 0.354	−0.004 ± 0.312	0.132 ± 0.295
VRT	0.036 ± 0.311	−0.068 ± 0.332	−0.131 ± 0.493
Absolute directional errors, cm			
|LNG|	0.321 ± 0.246	0.412 ± 0.314	0.341 ± 0.275
|LAT|	0.264 ± 0.237	0.240 ± 0.199	0.239 ± 0.218
|VRT|	0.246 ± 0.195	0.266 ± 0.211	0.385 ± 0.335
3D vector magnitude, cm	0.558 ± 0.275	0.626 ± 0.299	0.659 ± 0.350

Footnote: Data are presented as mean ± standard deviation (SD). Groups A, B, and C included 100, 100, and 55 patients, contributing 2,436, 2,468, and 1,351 CBCT registrations, respectively. Absolute directional deviations were calculated as the absolute values of signed deviations. The 3D vector magnitude was calculated as $\sqrt{(LNG^2 + LAT^2 + VRT^2)}$. CBCT, cone-beam computed tomography; LNG, longitudinal; LAT, lateral; VRT, vertical; 3D, three-dimensional.

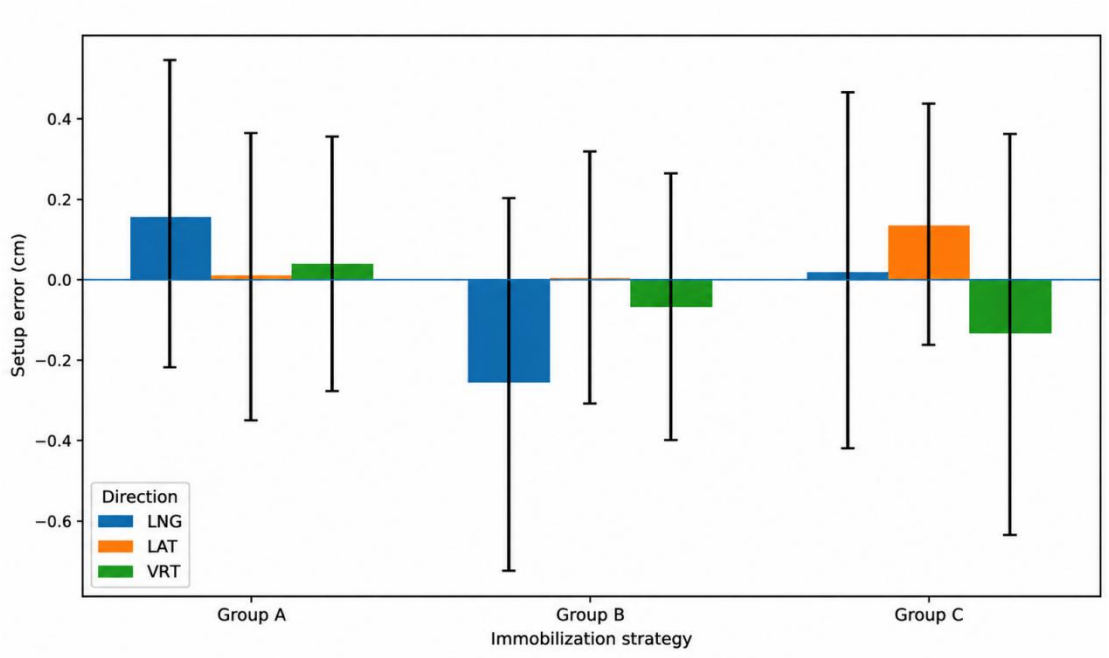


Figure 2. Signed CBCT-derived translational setup deviations by positioning–immobilization strategy.

Bars represent mean ± standard deviation of pre-correction LNG, LAT, and VRT deviations from daily CBCT registrations. Group A, supine with vacuum cushion; Group B, prone with Orfit frame and thermoplastic fixation; Group C, prone with individualized belly-board.

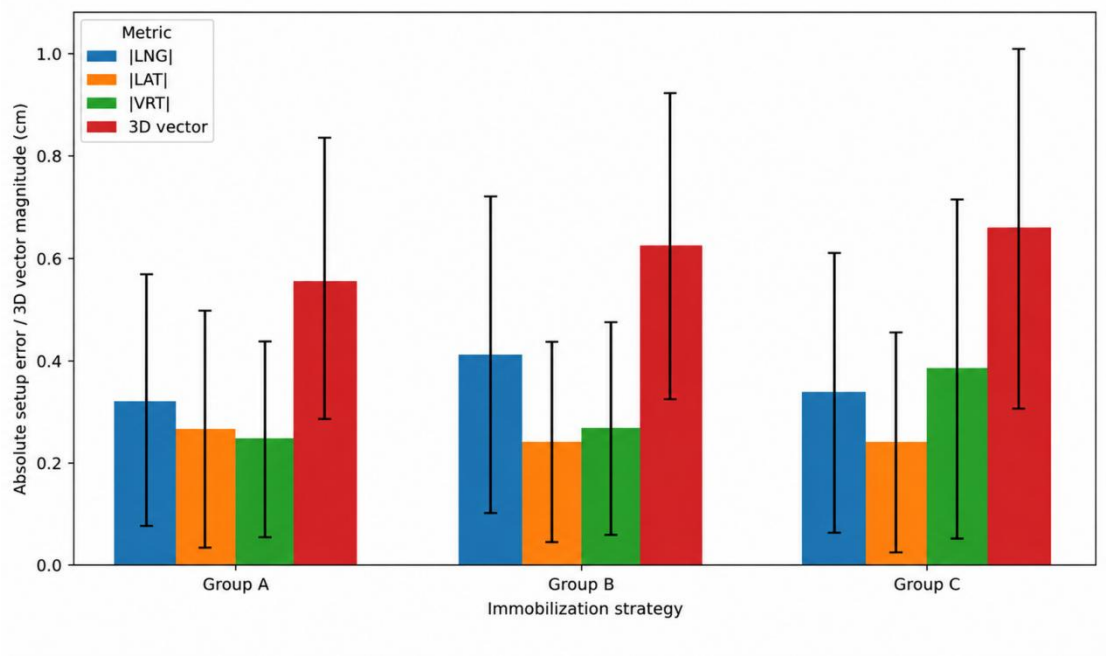


Figure 3. Absolute CBCT-derived translational setup deviations and 3D vector magnitude by positioning–immobilization strategy.

Bars represent mean ± standard deviation of absolute LNG, LAT, VRT, and 3D vector deviations from daily CBCT registrations. The 3D vector magnitude was calculated as $\sqrt{(LNG^2 + LAT^2 + VRT^2)}$. Group A, supine with vacuum cushion; Group B, prone with Orfit frame and thermoplastic fixation; Group C, prone with individualized belly-board.

3.3 Repeated-Measures GEE Analysis of CBCT-Derived Setup Deviations

Generalized estimating equation (GEE) models were used to assess associations between positioning–immobilization strategy and daily pre-correction CBCT-derived setup deviations while accounting for within-patient correlation. Group A served as the reference category, and treatment fraction was treated as a continuous variable. The primary outcome was 3D vector magnitude, with additional adjustment for age, BMI, and irradiation field extent in the multivariable model. Results are presented in Table 3.

3.3.1 Primary Outcome: 3D Vector Magnitude

In the unadjusted GEE analysis of 6,255 CBCT registrations from 255 patients, Groups B and C exhibited greater 3D vector magnitudes than Group A (Group B: β = 0.0675 cm, 95% CI 0.0171–0.1179, P = 0.009; Group C: β = 0.1016 cm, 95% CI 0.0379–0.1654, P = 0.002).

These associations remained significant in the multivariable analysis of 205 patients and 5,031 CBCT registrations after adjustment for age, BMI, and irradiation field extent (Group B: β = 0.0647 cm, 95% CI 0.0077–0.1217, P = 0.026; Group C: β = 0.1038 cm, 95% CI 0.0342–0.1734, P = 0.003).

Treatment fraction was positively associated with 3D vector magnitude in the adjusted model (β = 0.0032 cm/fraction, 95% CI 0.0018–0.0047, P < 0.001). Group-by-fraction interactions were not statistically significant (Group B × fraction: P = 0.348; Group C × fraction: P = 0.300), providing no evidence of different longitudinal slopes among the three groups.

3.3.2 Direction-Specific Absolute Setup Deviations

Direction-specific GEE analyses showed that Group B had greater absolute LNG deviation than Group A (β = 0.0906 cm, 95% CI 0.0417–0.1396, P < 0.001), whereas

Group C had greater absolute VRT deviation (β = 0.1399 cm, 95% CI 0.0763–0.2036, P < 0.001). No significant differences were observed for absolute LAT deviation or the remaining between-group comparisons.

Absolute LAT and VRT deviations increased with treatment fraction (LAT: β = 0.0021 cm/fraction, 95% CI 0.0012–0.0030, P < 0.001; VRT: β = 0.0022 cm/fraction, 95% CI 0.0010–0.0034, P < 0.001), whereas absolute LNG deviation showed no significant association (β = 0.0005 cm/fraction, 95% CI −0.0005 to 0.0016, P = 0.306).

Figure 4 illustrates the observed mean 3D vector magnitude across treatment-fraction intervals for each positioning–immobilization group.

Table 3. Generalized estimating equation analysis of daily CBCT-derived setup deviations

Outcome / Model term	**β (cm)**	**Robust SE**	**95% CI**	**P value**
3D vector magnitude — unadjusted model (n=255)				
Group B vs Group A	0.0675	0.0257	0.0171 to 0.1179	0.009
Group C vs Group A	0.1016	0.0325	0.0379 to 0.1654	0.002
Treatment fraction	0.0033	0.0007	0.0020 to 0.0046	<0.001
3D vector magnitude — adjusted model (n=205)				
Group B vs Group A	0.0647	0.0291	0.0077 to 0.1217	0.026
Group C vs Group A	0.1038	0.0355	0.0342 to 0.1734	0.003
Treatment fraction	0.0032	0.0008	0.0018 to	<0.001

			0.0047	
Age	−0.0003	0.0012	−0.0026 to 0.0020	0.793
BMI	0.0049	0.0042	−0.0033 to 0.0131	0.239
Extended irradiation field	0.0338	0.0318	−0.0285 to 0.0961	0.287
Absolute LNG deviation — unadjusted model (n=255)				
Group B vs Group A	0.0906	0.0250	0.0417 to 0.1396	<0.001
Group C vs Group A	0.0208	0.0217	−0.0218 to 0.0633	0.339
Treatment fraction	0.0005	0.0005	−0.0005 to 0.0016	0.306
Absolute LAT deviation — unadjusted model (n=255)				
Group B vs Group A	−0.0230	0.0168	−0.0560 to 0.0100	0.171
Group C vs Group A	−0.0251	0.0209	−0.0660 to 0.0159	0.230
Treatment fraction	0.0021	0.0005	0.0012 to 0.0030	<0.001
Absolute VRT deviation — unadjusted model (n=255)				
Group B vs Group A	0.0203	0.0193	−0.0175 to 0.0580	0.293
Group C vs Group A	0.1399	0.0325	0.0763 to 0.2036	<0.001

Treatment fraction	0.0022	0.0006	0.0010 to 0.0034	<0.001

Footnote: β coefficients represent estimated mean differences relative to Group A or changes per additional treatment fraction. All models used generalized estimating equations with a Gaussian distribution, identity link, exchangeable working correlation structure, patient-level clustering, and robust standard errors. Group A served as the reference category. Unadjusted models included immobilization strategy and treatment fraction (255 patients; 6,255 CBCT registrations). The adjusted 3D model additionally included age, BMI, and irradiation field extent (205 patients; 5,031 registrations). Direction-specific analyses were considered secondary outcomes. CI, confidence interval; BMI, body mass index; LNG, longitudinal; LAT, lateral; VRT, vertical; 3D, three-dimensional.

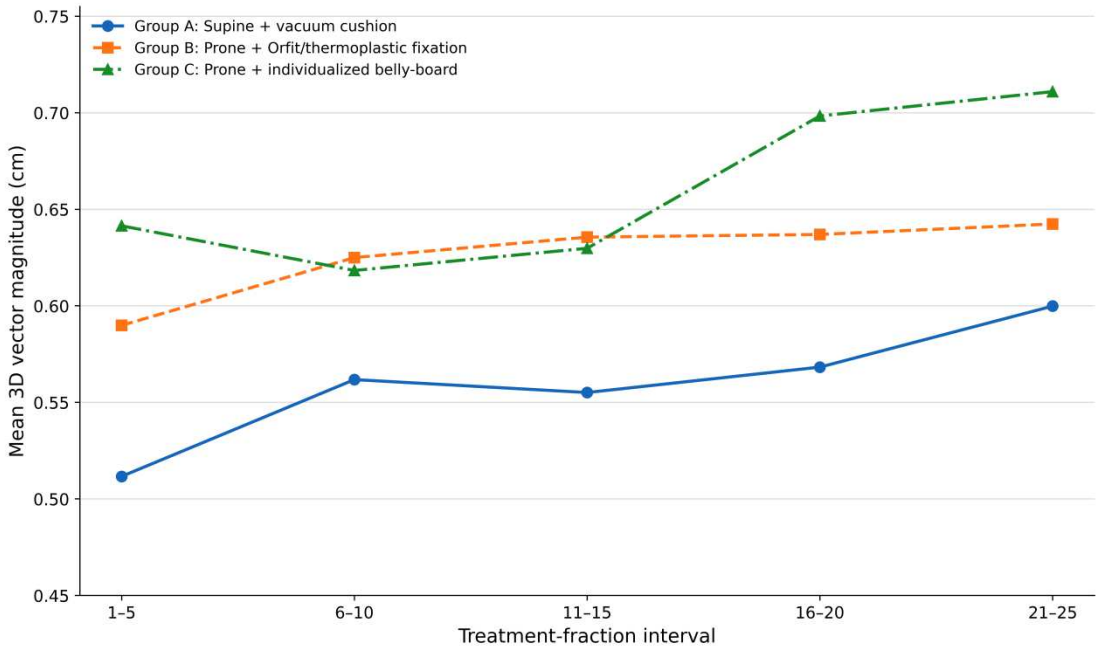


Figure 4. Mean 3D vector magnitude across treatment-fraction intervals by positioning–immobilization strategy.

Lines show the observed mean pre-correction 3D vector magnitude across five treatment-fraction intervals. Group A, supine with vacuum cushion; Group B, prone with Orfit frame and thermoplastic fixation; Group C, prone with individualized belly-board.

3.4 Patient-Level Sensitivity Analysis

To assess the robustness of the repeated-measures findings, a patient-level sensitivity analysis was performed using patient-specific summary measures, with each patient contributing one observation (Table 4).

Mean patient-level 3D vector magnitude differed among the three positioning–immobilization groups (P = 0.003), with values of 0.558 ± 0.175 cm, 0.626 ± 0.190 cm, and 0.660 ± 0.206 cm in Groups A, B, and C, respectively.

Direction-specific analyses showed significant overall between-group differences in mean absolute LNG and VRT deviations (both P < 0.001). Group B had the highest mean absolute LNG deviation (0.411 ± 0.194 cm), whereas Group C had the highest mean absolute VRT deviation (0.386 ± 0.224 cm). No significant difference was observed in mean absolute LAT deviation (P = 0.442).

The patient-specific 95th percentile of 3D vector magnitude also differed among the groups, with mean values of 0.861 ± 0.316 cm, 0.965 ± 0.293 cm, and 1.085 ± 0.348 cm in Groups A, B, and C, respectively (P < 0.001).

Overall, the patient-level analysis showed a pattern broadly consistent with the repeated-measures GEE findings, supporting the robustness of the observed between-group differences in 3D vector magnitude.

Table 4. Patient-level summary measures of CBCT-derived setup deviations used for sensitivity analysis

Outcome	Group A: Supine + vacuum cushion (n=100)	Group B: Prone + Orfit/thermoplastic fixation (n=100)	Group C: Prone + individualized belly-board (n=55)	H value	P value
Mean absolute LNG error (cm)	0.321 ± 0.158	0.411 ± 0.194	0.342 ± 0.112	14.472	<0.001

Mean absolute LAT error (cm)	0.263 ± 0.131	0.241 ± 0.106	0.239 ± 0.122	1.631	0.442
Mean absolute VRT error (cm)	0.246 ± 0.128	0.266 ± 0.145	0.386 ± 0.224	22.250	<0.001
Mean 3D vector error (cm)	0.558 ± 0.175	0.626 ± 0.190	0.660 ± 0.206	11.580	0.003
95th percentile 3D vector error (cm)	0.861 ± 0.316	0.965 ± 0.293	1.085 ± 0.348	21.156	<0.001

Footnote: Data are presented as mean ± standard deviation. Each patient contributed one summary observation based on daily pre-correction CBCT registrations. Between-group comparisons were performed using the Kruskal–Wallis test. LNG, longitudinal; LAT, lateral; VRT, vertical; 3D, three-dimensional; CBCT, cone-beam computed tomography.

3.5 Setup-Related Geometric Uncertainty and Descriptive Margin Estimates

Systematic (Σ) and random (σ) components of pre-correction CBCT-derived translational setup deviations were calculated for each positioning–immobilization strategy and direction (Table 5). Descriptive margin estimates were subsequently derived using the van Herk formula to compare setup-related geometric uncertainty among the groups.

Direction-specific patterns varied across the three strategies. Group B showed the largest descriptive margin estimate in the LNG direction (1.017 cm), whereas Group C showed the largest estimate in the VRT direction (1.174 cm) and the smallest estimate in the LAT direction (0.597 cm). In Group A, estimates ranged from 0.754 to

0.878 cm across the three directions.

As these estimates were based on pre-correction setup deviations and did not account for post-correction residual errors, anatomical changes, rotational errors, or intrafraction motion, they should be interpreted solely as descriptive measures of setup-related geometric uncertainty rather than recommended clinical CTV-to-PTV margins.

Table 5. Systematic and random components of pre-correction CBCT-derived setup deviations and descriptive margin estimates

Positioning–immobilization strategy	Direction	Systematic component, Σ (cm)	Random component, σ (cm)	Descriptive margin estimate (cm)
Group A	LNG	0.280	0.255	0.878
	LAT	0.240	0.267	0.787
	VRT	0.247	0.195	0.754
Group B	LNG	0.314	0.331	1.017
	LAT	0.207	0.240	0.686
	VRT	0.262	0.212	0.804
Group C	LNG	0.249	0.370	0.882
	LAT	0.170	0.247	0.597
	VRT	0.376	0.332	1.174

Footnote: Σ was defined as the standard deviation of patient-specific mean setup deviations, and σ as the root-mean-square of patient-specific standard deviations. Descriptive margin estimates were calculated using $M = 2.5\Sigma + 0.7\sigma$ based on pre-correction CBCT data and should not be interpreted as recommended clinical CTV-to-PTV margins. LNG, longitudinal; LAT, lateral; VRT, vertical; CBCT, cone-beam computed tomography.

3.6 Treatment-Course Setup Reproducibility

Treatment-course setup reproducibility was evaluated using two complementary threshold-based measures derived from pre-correction translational setup deviations in

all three directions (LNG, LAT, and VRT): (1) a strict patient-level criterion, defined as meeting the specified threshold in all three directions simultaneously at every available pretreatment CBCT verification throughout the treatment course, and (2) the patient-specific fraction pass rate, defined as the proportion of available treatment fractions in which all three directional deviations simultaneously met the corresponding threshold for each patient (Table 6 and Figure 5). The 0.5-cm and 1.0-cm thresholds were used as prespecified descriptive benchmarks for comparing pretreatment setup reproducibility and were not intended to represent clinical action levels or recommended setup tolerances.

Using the ≤0.5-cm threshold, the strict patient-level criterion was met by 43.0%, 28.0%, and 12.7% of patients in Groups A, B, and C, respectively ($P < 0.001$). Using the ≤1.0-cm threshold, the corresponding proportions were 78.0%, 63.0%, and 61.8%, respectively ($P = 0.034$).

Patient-specific fraction pass rates showed a similar between-group pattern. For the ≤0.5-cm threshold, mean fraction pass rates were 76.0%, 63.6%, and 57.6% in Groups A, B, and C, respectively ($P < 0.001$). For the ≤1.0-cm threshold, the corresponding rates were 97.4%, 94.9%, and 93.6%, respectively ($P = 0.024$).

Descriptively, Group A showed the highest strict patient-level attainment proportions and mean patient-specific fraction pass rates across both thresholds. Because these measures were derived from pre-correction CBCT-derived translational setup deviations obtained from routine clinical registration, they should be interpreted as descriptive measures of pretreatment setup reproducibility rather than direct measures of isolated immobilization-device stability, post-correction treatment accuracy, or target-position reproducibility. Furthermore, because the group-by-treatment-fraction interaction was not statistically significant in the repeated-measures analysis, these findings should not be interpreted as evidence of different longitudinal rates of change in setup deviation among the three positioning–immobilization strategies.

Table 6. Treatment-course setup reproducibility based on three-directional translational setup-error thresholds

A. Strict patient-level threshold attainment

Stability criterion	Group A (n=100)	Group B (n=100)	Group C (n=55)	P value
All three absolute directional deviations ≤0.5 cm	43 (43.0%)	28 (28.0%)	7 (12.7%)	<0.001
All three absolute directional deviations ≤1.0 cm	78 (78.0%)	63 (63.0%)	34 (61.8%)	0.034

B. Patient-specific fraction pass rates based on three-directional thresholds

Outcome	Group A	Group B	Group C	H value	P value
Three-directional threshold ≤0.5 cm (%)	76.0 ± 27.5	63.6 ± 29.6	57.6 ± 26.6	17.36	<0.001
Three-directional threshold ≤1.0 cm (%)	97.4 ± 6.9	94.9 ± 9.3	93.6 ± 12.7	7.48	0.024

Footnote: Threshold attainment required the absolute translational deviations in all three directions (LNG, LAT, and VRT) to simultaneously meet the specified threshold. Strict patient-level attainment required this criterion at every available pretreatment CBCT verification, whereas patient-specific fraction pass rates represented the percentage of fractions meeting the criterion. Between-group comparisons used the chi-square or Fisher's exact test and the Kruskal–Wallis test, respectively. These measures reflect pretreatment setup reproducibility rather than immobilization-device stability or post-correction accuracy. CBCT, cone-beam computed tomography.

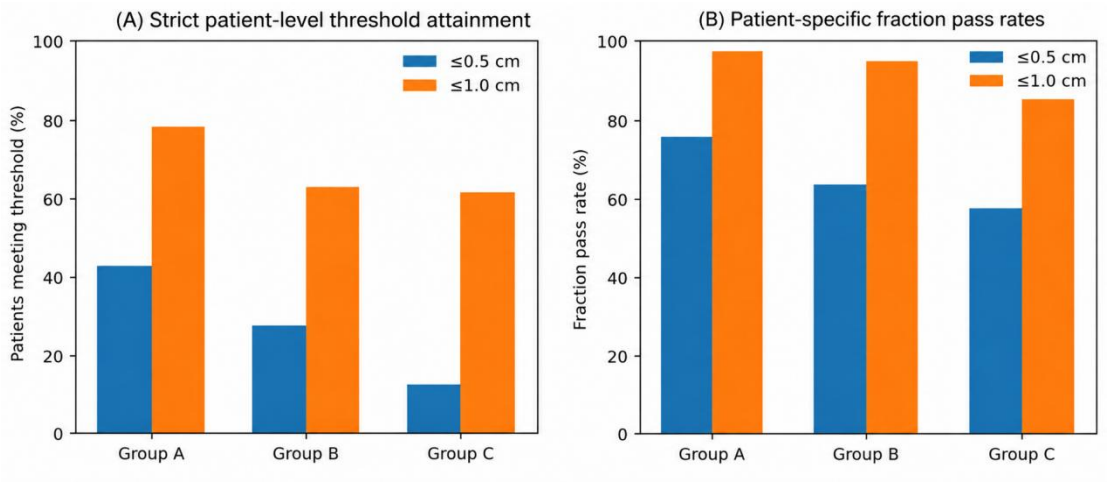


Figure 5. Treatment-course setup reproducibility based on three-directional translational setup-error thresholds.

(A) Strict patient-level threshold attainment. (B) Mean patient-specific fraction pass rates. Threshold attainment required the absolute translational deviations in all three directions (LNG, LAT, and VRT) to simultaneously meet the specified threshold. Strict patient-level attainment required this criterion at every available pretreatment CBCT verification.

4. Discussion

The present study provides a longitudinal evaluation of pretreatment setup reproducibility among three combined positioning–immobilization strategies for cervical cancer VMAT, based on 6,255 daily pretreatment CBCT registrations from 255 patients. Using generalized estimating equations (GEE) to account for within-patient correlation, we identified significant between-group differences in pre-correction CBCT-derived setup deviations. In the adjusted analysis, Groups B and C showed greater 3D vector magnitudes than Group A ($\beta = 0.0647$ cm, $P = 0.026$; and $\beta = 0.1038$ cm, $P = 0.003$, respectively). Supine positioning with vacuum-cushion immobilization was associated with lower 3D vector magnitudes than the two prone positioning–immobilization strategies, while direction-specific analyses demonstrated distinct patterns of longitudinal and vertical deviations among the groups. A modest increase in 3D vector magnitude was observed over the treatment course; however, the absence of significant group-by-fraction interactions indicated that the longitudinal pattern of change did not differ significantly among the three strategies.

Previous studies have used CBCT and other image-guidance approaches to characterize interfractional setup deviations, systematic and random uncertainties, and positioning reproducibility during cervical cancer radiotherapy [14–16]. The present study builds on this existing evidence by using a relatively large daily pretreatment CBCT dataset together with repeated-measures modeling and complementary patient-level sensitivity analyses to characterize pretreatment setup reproducibility across the radiotherapy course.

Previous studies have also directly compared positioning and immobilization approaches in cervical cancer radiotherapy. Li et al. compared vacuum-bag fixation with Orfit rack and thermoplastic membrane fixation using CBCT-based image guidance and reported direction-specific differences in setup deviations [17]. Xiao et al. analyzed 3,642 daily iterative CBCT registrations from 132 patients with cervical cancer undergoing VMAT, demonstrating the utility of repeated daily image guidance for characterizing setup errors [18]. More recently, Lin et al. compared three positioning–immobilization approaches broadly corresponding to those evaluated in the present study, including a supine vacuum-bag system, a prone Orfit Rack, and a personalized prone-plate system, using daily fan-beam CT [19]. Collectively, these studies demonstrate that comparisons of positioning and immobilization approaches using repeated image guidance have already been undertaken in cervical cancer radiotherapy. The added value of the present study therefore lies primarily in the relatively large longitudinal daily-CBCT dataset and the use of a repeated-measures GEE framework to explicitly account for within-patient correlation, complemented by patient-level sensitivity analyses. This analytical framework provides additional longitudinal evidence regarding pretreatment setup reproducibility across different positioning–immobilization strategies rather than establishing the superiority of any individual immobilization device.

The lower pre-correction setup deviations observed in Group A may reflect the combined influence of treatment position, immobilization configuration, anatomical support, patient–device interaction, and other clinical or workflow-related factors. Supine positioning with vacuum-cushion immobilization provides individualized

support for the trunk, pelvis, and lower extremities and may facilitate reproducible repositioning during repeated treatment sessions. In contrast, prone positioning involves different patterns of abdominal support, pelvic orientation, lower-extremity positioning, and body-surface contact, which may contribute to distinct direction-specific setup deviations. Previous comparative studies have similarly suggested that treatment position and immobilization configuration may influence setup reproducibility, although the magnitude and direction of these differences vary according to the technique, study population, and image-registration approach [20–22]. Importantly, because treatment position and immobilization method differed simultaneously among the three groups in the present retrospective cohort, the independent contributions of these individual components cannot be separated. The observed differences should therefore be interpreted as associations with the combined positioning–immobilization strategies rather than as evidence of an independent effect or superiority of the vacuum cushion, Orfit body frame, belly-board, or treatment position itself.

Direction-specific analyses further revealed distinct patterns of pre-correction setup deviation among the three positioning–immobilization strategies. Group B, which combined prone positioning with an Orfit body frame and thermoplastic fixation, showed a greater absolute LNG deviation than Group A in the repeated-measures analysis. The cranio-caudal direction may be particularly sensitive to differences in whole-body positioning, including variations in pelvic orientation, trunk extension, and lower-extremity placement between treatment fractions. In the prone position, reproducible longitudinal alignment requires consistent repositioning of multiple anatomical support points along the body, which may contribute to greater interfraction variation in this direction. Previous work by Zheng et al. similarly reported differences in longitudinal setup uncertainty between prone and supine positioning during pelvic radiotherapy, supporting the potential relevance of treatment posture to direction-specific setup reproducibility [23]. Nevertheless, because the present study did not directly quantify pelvic rotation, body extension, or lower-extremity displacement, these potential mechanisms remain explanatory

hypotheses rather than directly measured causes of the observed LNG differences.

A different direction-specific pattern was observed in Group C, which combined prone positioning with an individualized belly-board system. Group C showed a greater absolute VRT deviation than Group A in the repeated-measures analysis, suggesting greater pre-correction variability in the vertical direction for this positioning–immobilization strategy. One possible explanation is that vertical reproducibility in the prone position may be influenced by the consistency of abdominal support, body-surface contact, pelvic orientation, and patient positioning within the support system across treatment fractions. Changes in abdominal configuration, body contour, or patient relaxation could potentially alter the vertical relationship between the pelvis and the support surface. Previous studies have emphasized the importance of reproducible patient–immobilization-device contact and body support for setup reproducibility during pelvic radiotherapy [24]. However, these anatomical and mechanical factors were not directly measured in the present study, and the greater VRT deviation observed in Group C therefore cannot be attributed specifically to the belly-board itself. Taken together, the direction-specific findings suggest that pretreatment setup reproducibility may reflect the combined influence of treatment position, immobilization configuration, patient support, and interfraction patient-related variation rather than the mechanical characteristics of an individual immobilization device alone.

A methodological strength of the present study is the use of generalized estimating equations (GEE) to account for within-patient correlation across repeated daily CBCT measurements. This approach provided population-averaged estimates of associations between positioning–immobilization strategy, treatment fraction, and pre-correction setup deviations while accommodating repeated and potentially unbalanced observations within patients [25,26].

Beyond the evaluation of mean translational setup deviations, the present study also quantified systematic (Σ) and random (σ) components of pre-correction setup uncertainty for each positioning–immobilization strategy. These parameters provide complementary information regarding the magnitude and pattern of geometric setup

uncertainty beyond mean directional deviations alone [27,28]. Descriptive margin estimates calculated using the van Herk formula further illustrated direction-specific differences among the three strategies, including greater longitudinal uncertainty in Group B and greater vertical uncertainty in Group C. However, these estimates were derived exclusively from pre-correction CBCT-derived translational setup deviations obtained from routine clinical registration and did not incorporate post-correction residual uncertainty, target motion or deformation, rotational error, or intrafraction motion. Accordingly, they should be interpreted as comparative descriptors of setup-related geometric uncertainty rather than as recommended clinical CTV-to-PTV margins for a daily image-guided workflow and are not intended for direct application in clinical treatment planning.

Daily image guidance enables translational deviations identified on pretreatment imaging to be corrected before treatment delivery, but minimizing the magnitude and variability of initial setup deviations remains relevant to treatment workflow and geometric reproducibility. Systematic and random components provide complementary information regarding patterns of setup uncertainty, while rotational errors and other geometric uncertainties not captured by translational correction may remain relevant in highly conformal radiotherapy [29]. In the present study, the routine clinical registration workflow was based on three translational degrees of freedom (LNG, LAT, and VRT), and rotational registration and correction were not routinely performed. Consequently, rotational setup errors were not available for systematic analysis. Routine post-correction CBCT was also not performed, and intrafraction motion and target-level residual uncertainty were not evaluated. Therefore, the observed differences in pre-correction setup reproducibility should not be interpreted as direct evidence of differences in post-correction treatment accuracy, cumulative dose delivery, or target coverage.

Setup reproducibility may also vary over the course of cervical cancer radiotherapy, which is delivered over several weeks and may be accompanied by progressive anatomical and physiological changes. Variations in body weight, external body contour, bladder filling, and rectal filling have been reported as potential

692 contributors to interfraction geometric variation during pelvic radiotherapy [30,31]. In
693 the present study, treatment fraction number was positively associated with 3D vector
694 magnitude, indicating a modest increase in pre-correction setup deviation over the
695 treatment course. However, no significant group-by-fraction interaction was identified,
696 suggesting that the longitudinal pattern did not differ significantly among the three
697 positioning–immobilization strategies. These findings support consideration of setup
698 reproducibility as a longitudinal rather than purely single-fraction characteristic, while
699 the specific anatomical or physiological mechanisms underlying the observed
700 temporal change could not be determined from the present dataset.

701 The threshold-based analyses provided a complementary description of
702 treatment-course setup reproducibility. At the ≤0.5-cm threshold, strict patient-level
703 attainment rates were 43.0%, 28.0%, and 12.7% in Groups A, B, and C, respectively
704 ($P < 0.001$), whereas the corresponding rates at the ≤1.0-cm threshold were 78.0%,
705 63.0%, and 61.8% ($P = 0.034$). Mean patient-specific fraction pass rates were also
706 highest in Group A at both thresholds. Threshold attainment required the absolute
707 translational deviations in all three directions (LNG, LAT, and VRT) to
708 simultaneously meet the specified criterion. These findings were broadly consistent
709 with the repeated-measures and patient-level analyses. However, the thresholds were
710 intended as descriptive benchmarks rather than clinical action levels or recommended
711 PTV margins. Moreover, because the three groups differed in both treatment position
712 and immobilization configuration, these differences cannot be attributed to the
713 immobilization devices alone.

714 The clinical relevance of pretreatment setup reproducibility should be considered
715 within the broader context of modern image-guided VMAT. Although the
716 between-group differences in 3D vector magnitude were statistically significant, their
717 absolute magnitudes were small (approximately 0.06–0.10 cm in the adjusted
718 analysis), and the clinical significance of differences of this magnitude remains
719 uncertain in the context of daily CBCT-guided translational correction. Highly
720 conformal treatment techniques rely on consistent patient positioning and image
721 guidance to support accurate treatment delivery [32]. Nevertheless, the present study

evaluated only pre-correction CBCT-derived translational setup deviations obtained from routine clinical registration and did not assess target position, target coverage, rotational errors, intrafraction motion, post-correction residual uncertainty, or delivered dose. Accordingly, the observed between-group differences cannot establish whether one positioning–immobilization strategy permits smaller clinical PTV margins or provides superior target coverage or organ-at-risk sparing. This distinction is particularly important in cervical cancer radiotherapy, where bowel and other pelvic-organ exposure is clinically relevant to treatment-related toxicity and quality of life [33,34]. Future studies integrating daily image guidance with target-level soft-tissue assessment, rotational and residual setup measurements, intrafraction monitoring, and accumulated dosimetric evaluation will be needed to determine whether differences in pretreatment setup reproducibility translate into meaningful dosimetric or clinical benefits.

As image-guided and adaptive radiotherapy techniques continue to evolve, reproducible patient positioning remains an important component of the overall treatment workflow [35,36]. However, the present findings are limited to pre-correction CBCT-derived translational setup reproducibility and should not be extrapolated to post-correction treatment accuracy or the dosimetric or clinical performance of adaptive radiotherapy.

The present study has several methodological strengths. First, the relatively large dataset included 255 consecutive patients and 6,255 daily pretreatment CBCT registrations, enabling setup reproducibility to be evaluated longitudinally across the radiotherapy course rather than on the basis of a limited number of imaging fractions. Second, repeated-measures GEE models were used to account for within-patient correlation arising from daily CBCT measurements, together with multivariable adjustment for available potential confounders and complementary patient-level sensitivity analyses to assess the robustness of the observed between-group patterns. Third, the analysis incorporated multiple complementary measures of pre-correction setup reproducibility, including signed and absolute directional deviations, 3D vector magnitude, systematic and random components, longitudinal changes across treatment

752 fractions, descriptive margin estimates, and patient-level threshold-based measures.
753 Collectively, these analyses provide a detailed characterization of pre-correction setup
754 reproducibility among three combined positioning–immobilization strategies used in
755 routine cervical cancer VMAT.

756 Several limitations should also be acknowledged. First, this was a retrospective
757 single-center study, and the positioning–immobilization strategies were selected
758 according to routine clinical practice rather than randomized allocation. Although the
759 multivariable analyses adjusted for available clinically relevant covariates, including
760 age, BMI, and irradiation field extent, detailed disease- and treatment-related
761 characteristics were not systematically available in the retrospective setup database.
762 Therefore, residual selection bias and unmeasured confounding cannot be excluded,
763 and the observed between-group differences should be interpreted as associations
764 rather than causal effects of the positioning–immobilization strategies. In addition, the
765 adjusted GEE analysis was restricted to 205 patients with complete covariate data,
766 primarily because of missing BMI information. As BMI availability differed among
767 the three groups, potential selection bias associated with complete-case analysis
768 cannot be excluded.

769 Second, the routine clinical CBCT registration procedure incorporated
770 information from the PTV, relevant soft-tissue anatomy, and pelvic bony structures
771 rather than using an exclusively bone-based registration protocol. Consequently, the
772 recorded pre-correction translational setup deviations may reflect both external
773 positioning variation and internal anatomical changes and should not be interpreted as
774 a pure measure of immobilization reproducibility. A retrospective bone-only
775 re-registration of all CBCT datasets and a formal assessment of interobserver
776 registration reproducibility were not available in the present study. In addition, both
777 the planning CT and CBCT images had a slice thickness of 5 mm, which may have
778 limited spatial resolution in the longitudinal direction and potentially influenced the
779 precision of longitudinal registration, although the same imaging protocol was applied
780 across all three groups.

781 Third, the routine clinical registration workflow used three translational degrees

of freedom without rotational registration or correction; therefore, rotational setup errors were not available for systematic evaluation. Post-correction residual errors, intrafraction motion, daily uterus/cervix position or deformation, target–PTV relationships, and their dosimetric consequences were also not comprehensively evaluated. Consequently, translation-only analysis may not capture the full geometric uncertainty relevant to treatment delivery, and the present findings cannot directly establish target-position reproducibility, post-correction treatment accuracy, target coverage, or clinical CTV-to-PTV margin requirements.

Fourth, patient-centered and workflow-related outcomes, including treatment comfort, setup time, workflow efficiency, and patient-reported experience, were not assessed and may also influence the clinical applicability of different positioning–immobilization strategies. Finally, prospective multicenter studies incorporating standardized registration protocols, target-level assessment, six-degree-of-freedom geometric evaluation, post-correction verification, intrafraction monitoring, and comprehensive dosimetric analysis are warranted to further validate these findings.

5. Conclusions

The three positioning–immobilization strategies demonstrated distinct patterns of pre-correction setup reproducibility during daily CBCT-guided VMAT for cervical cancer. Supine positioning with vacuum-cushion immobilization was associated with smaller 3D vector magnitudes and higher three-directional threshold-attainment rates than the two prone strategies. Although setup deviations increased modestly over the treatment course, longitudinal trends did not differ significantly among groups. These findings reflect differences in pretreatment setup reproducibility rather than isolated immobilization-device superiority, post-correction treatment accuracy, or clinical PTV-margin requirements.

Declarations

Abbreviations

3D, three-dimensional; BMI, body mass index; CBCT, cone-beam computed tomography; CI, confidence interval; CTV, clinical target volume; GEE, generalized estimating equation; IGRT, image-guided radiotherapy; IQR, interquartile range; LAT,

lateral; LNG, longitudinal; PTV, planning target volume; SD, standard deviation; VMAT, volumetric modulated arc therapy; VRT, vertical; Σ, systematic error; σ, random error.

Ethics approval and consent to participate

This study was approved by the Ethics Committee of Sun Yat-sen University Cancer Center (Approval No. SL-B2024-773-02) and was conducted in accordance with the Declaration of Helsinki. The requirement for informed consent was waived by the Ethics Committee of Sun Yat-sen University Cancer Center owing to the retrospective nature of the study.

Consent for publication

Not applicable.

Availability of data and materials

The datasets generated and/or analyzed during the current study are available from the corresponding author upon reasonable request.

Competing interests

The authors declare that they have no competing interests.

Funding

This work was supported by the Research Fund of the Department of Radiation Oncology, Sun Yat-sen University Cancer Center, for the project “Evaluation System for Radiotherapy Immobilization Devices Based on a Nomogram Model” (Grant No. PT02128001).

Authors' contributions

Zhiyue Lin, Hailong Wang, and Yingnan Qi contributed equally to this work and were involved in the study conception and design, data collection, data analysis, data interpretation, and manuscript drafting. Kai Wang, Jiaxiu Luo, and Zongtai Li were responsible for clinical data collection, data organization, and database management. Bin Zhang and Senkui Xu contributed to statistical analysis, figure preparation, and graphical presentation. Huilang He, Feng Chi, and Wenlong Zhu provided methodological guidance, supervised the study, and critically reviewed and revised the manuscript. Huilang He, Feng Chi, and Wenlong Zhu served as corresponding

authors. All authors read and approved the final manuscript.

Acknowledgements

Not applicable.

Clinical trial registration

Not applicable. This study was a retrospective observational analysis of routinely collected clinical data. No prospective assignment of participants to study-related interventions was performed.

[1] Bhatla N, Aoki D, Sharma DN, Sankaranarayanan R. Cancer of the cervix uteri: 2021 update. Int J Gynaecol Obstet. 2021;155(Suppl 1):28-44. doi:10.1002/ijgo.13865

[2] Sung H, Ferlay J, Siegel RL, et al. Global cancer statistics 2020: GLOBOCAN estimates of incidence and mortality worldwide for 36 cancers in 185 countries. CA Cancer J Clin. 2021;71(3):209-249. doi:10.3322/caac.21660

[3] Chargari C, Peignaux K, Escande A, et al. Radiotherapy of cervical cancer. Cancer Radiother. 2022;26(1-2):298-308. doi:10.1016/j.canrad.2021.11.009

[4] Faye MD, Alfieri J. Advances in radiation oncology for the treatment of cervical cancer. Curr Oncol. 2022;29(2):928-944. doi:10.3390/curroncol29020079

[5] Van Herk M. Errors and margins in radiotherapy. Semin Radiat Oncol. 2004;14(1):52-64. doi:10.1053/j.semradonc.2003.10.003

[6] Van Herk M, Remeijer P, Rasch C, Lebesque JV. The probability of correct target dosage: dose-population histograms for deriving treatment margins in radiotherapy. Int J Radiat Oncol Biol Phys. 2000;47(4):1121-1135. doi:10.1016/S0360-3016(00)00518-6

[7] Cubillos-Mesías M, Boda-Heggemann J, Thoelking J, et al. Quantification and assessment of interfraction setup errors based on cone-beam CT and determination of safety margins for radiotherapy. PLoS One. 2016;11(3):e0150326. doi:10.1371/journal.pone.0150326

[8] Xiao N, Yuan C, Zhao T, et al. Comparative impact of supine vs prone positioning on dose distribution, acute toxicity, and setup error in postoperative radiotherapy for cervical cancer: a multidimensional propensity-matched cohort study. Front Oncol. 2025;15:1637443. doi:10.3389/fonc.2025.1637443

[9] Patni N, Burela N, Pasricha R, et al. Assessment of three-dimensional setup errors in image-guided pelvic radiotherapy for uterine and cervical cancer using kilovoltage cone-bea

m computed tomography and its effect on planning target volume margins. J Cancer Res Ther. 2017;13(1):131-136. doi:10.4103/0973-1482.199449

[10] Anghel B, Serboiu C, Marinescu A, et al. Recent advances and adaptive strategies in image guidance for cervical cancer radiotherapy. Medicina (Kaunas). 2023;59(10):1735. doi:10.3390/medicina59101735

[11] Anand M, Parikh A, Shah SP. Comparison of thermoplastic masks and knee wedge as immobilization devices for image-guided pelvic radiation therapy using Cone Beam Computed Tomography. Indian J Cancer. 2020;57(2):182-186. doi:10.4103/ijc.IJC_602_18

[12] Ruan J, Huang X, Wang T, et al. Impact of belly board immobilization devices and body mass factor on setup displacement using daily cone-beam CT in rectal cancer radiotherapy. J Appl Clin Med Phys. 2025;26(3):e14573. doi:10.1002/acm2.14573

[13] Zeng Z, Zhu J, Wang Z, et al. Pelvic target volume inter-fractional motion during radiotherapy for cervical cancer with daily iterative cone-beam computed tomography. Radiat Oncol. 2024;19:55. doi:10.1186/s13014-024-02438-1

[14] Sagae S, Toita T, Matsuura M, et al. Improvement in radiation techniques for locally advanced cervical cancer during the last two decades. Int J Gynecol Cancer. 2023;33(8):1295-1303. doi:10.1136/ijgc-2022-004230

[15] Wakabayashi K, Hirata M, Monzen H, et al. Optimal correction strategy of image-guided radiation therapy including the para-aortic lymph node region in patients with cervical cancer. Adv Radiat Oncol. 2024;9(12):101643. doi:10.1016/j.adro.2024.101643

[16] Zhang Y, Wang Y, Zhang W, et al. Prospects for daily online adaptive radiotherapy for cervical cancer: auto-contouring evaluation and dosimetric outcomes. Radiat Oncol. 2024;19:7. doi:10.1186/s13014-024-02398-6

[17] Li YB, Wang YL, Zhuo YH. Comparison of vacuum bag fixation and Orfit rack with thermoplastic membrane fixation for image-guided cervical cancer radiotherapy. Zhonghua Zhong Liu Za Zhi. 2017;39(6):467-470. doi:10.3760/cma.j.issn.0253-3766.2017.06.012.

[18] Xiao H, Han Q, Wei S, et al. Setup errors analysis in iterative kV CBCT: A clinical study of cervical cancer treated with Volumetric Modulated Arc Therapy. J Appl Clin Med Phys. 2024;25(10):e14480. doi:10.1002/acm2.14480.

[19] Lin X, Piao Z, Huang X, et al. Inter-fraction target and OARs reproducibility in cerv

902 ical cancer: Influence of immobilization systems and patient positioning verified by daily f
903 an beam CT. Radiography (Lond). 2026;32(3):103328. doi:10.1016/j.radi.2026.103328.
904 [20] Virkar M, Kumar NA, Chadha P, Rodrigues RJ, Kharde A. Vacuum and thermoplasti
905 c mould-based immobilization systems used in patients undergoing pelvic radiation therapy:
906 a comparative study. Int J Clin Biomed Res. 2020;6(1):8-10. doi:10.31878/IJCBR.2019.61.
907 03
908 [21] Gao LJ, Huang JM, Huang J, et al. Comparison of setup errors between Orfit frame
909 and vacuum bag in radiotherapy for cervical cancer. Chin J Radiat Oncol. 2017;26(9):1080
910 -1083. doi:10.3760/cma.j.issn.1004-4221.2017.09.020
911 [22] Nambiar KKV, Sandhya G, Shadab A, et al. Comparison of thermoplastic cast versus
912 knee wedge/foot rest immobilization technique in uterine cervical carcinoma patients recei
913 ving radiotherapy. J Anal Oncol. 2022;11:64-70.
914 [23] Zheng Z, Liu D, Su Y. Supine/prone position fixation treatment in cervical cancer ra
915 diotherapy. J Cancer Res Ther. 2025;21(2):401-408. doi:10.4103/jcrt.jcrt_2050_24
916 [24] Li Y, Sun W, Liu S, et al. Effect of body contour changes on the setup and dosimet
917 ric accuracy of radiotherapy after cervical cancer surgery. Front Oncol. 2024;14:1392741. d
918 oi:10.3389/fonc.2024.1392741
919 [25] de Melo MB, Daldegan-Bueno D, Menezes Oliveira MG, et al. Beyond ANOVA and
920 MANOVA for repeated measures: advantages of generalized estimated equations and gene
921 ralized linear mixed models and its use in neuroscience research. Eur J Neurosci. 2022;56
922 (12):6089-6098. doi:10.1111/ejn.15858
923 [26] Ballinger GA. Using generalized estimating equations for longitudinal data analysis. O
924 rgan Res Methods. 2004;7(2):127-150. doi:10.1177/1094428104263672
925 [27] Mohamed R, Elawadi AA, Alkhanein N, Alharth M, Asiri M. Factors affecting isoce
926 nter displacement and planning target volume margin for patients with rectal cancer receivi
927 ng radiation therapy. Adv Radiat Oncol. 2022;7(6):101060. doi:10.1016/j.adro.2022.101060
928 [28] Li Z, Cheng Y, Dong J, et al. The impact of setup errors on dose distribution in cer
929 vical cancer radiotherapy and the margin from CTV to PTV. J Cancer Res Clin Oncol. 20
930 24;150:516. doi:10.1007/s00432-024-06032-6
931 [29] Tsujii K, Ueda Y, Isono M, Miyazaki M, Teshima T. Dosimetric impact of rotational

setup errors in volumetric modulated arc therapy for postoperative cervical cancer. J Radiat Res. 2021;62(4):688-697. doi:10.1093/jrr/rrab039

[30] Lee J, Chang CL, Lin JB, et al. The effect of body mass index and weight change on late gastrointestinal toxicity in locally advanced cervical cancer treated with intensity-modulated radiotherapy. Int J Gynecol Cancer. 2018;28(7):1377-1386. doi:10.1097/IGC.0000000000001312

[31] Ge BB, Liu Y, Jin JH, et al. Effect of bladder filling status on positioning errors in post-hysterectomy cervical cancer radiotherapy. Ann Med. 2023;55(2):2249936. doi:10.1080/07853890.2023.2249936

[32] Ding F, Zhang S, Liu D, et al. Comparison of clinical efficacy between volumetric modulated arc therapy and fixed-field intensity-modulated radiotherapy in the treatment of locally advanced cervical cancer. Zhonghua Zhong Liu Fang Zhi. 2023;30(7):424.

[33] Gao H, Wu H, Zhang Y, et al. Dose-volume constraints for severe acute gastrointestinal toxicity in cervical cancer patients receiving extended-field intensity-modulated radiotherapy and concurrent chemotherapy. Radiother Oncol. 2025;205:110777. doi:10.1016/j.radonc.2025.110777

[34] Padhi S, Mahapatra BR, Pati KC, et al. Comparison of Acute Gastrointestinal Toxicity of Intensity-Modulated Radiotherapy Versus Three-Dimensional Conformal Radiotherapy in Patients of Carcinoma Cervix. Cureus. 2023;15(11):e48876. Published 2023 Nov 16. doi:10.7759/cureus.48876

[35] Wang G, Wang Z, Zhang Y, et al. Daily online adaptive radiation therapy of postoperative endometrial and cervical cancer with PTV margin reduction to 5 mm: dosimetric outcomes, acute toxicity, and first clinical experience. Adv Radiat Oncol. 2024;9(7):101510. doi:10.1016/j.adro.2024.101510

[36] Wang H, Li Z, Shi D, et al. Assessing intra- and interfraction motion and its dosimetric impacts on cervical cancer adaptive radiotherapy based on 1.5T MR-Linac. Radiat Oncol. 2024;19:176. doi:10.1186/s13014-024-02569-5